

# Optimizing quasi-phase matching of high harmonic generation using counterpropagating pulse trains

Oren Cohen,\* Amy L. Lytle, Xiaoshi Zhang, Margaret M. Murnane, and Henry C. Kapteyn

JILA, University of Colorado, and National Institute of Standards and Technologies, Boulder, Colorado 80309, USA

\*Corresponding author: oren.cohen@colorado.edu

Received June 12, 2007; revised September 5, 2007; accepted September 5, 2007;  
posted September 13, 2007 (Doc. ID 83912); published October 8, 2007

We formulate a theory of quasi-phase matching of high harmonic generation using weak counterpropagating pulse trains. We predict the optimal laser intensities and pulse shapes for the counterpropagating field and find that the conversion efficiency is better than the efficiency obtained by simply suppressing harmonic emission from out-of-phase regions. © 2007 Optical Society of America

OCIS codes: 190.0190, 190.2620.

Quasi-phase matching (QPM) is a widely used technique in visible nonlinear optics. In materials where perfect phase matching is not possible, QPM makes it possible to obtain significant conversion efficiency in a nonlinear process by periodically varying the nonlinear susceptibility of a material [1]. In high harmonic generation (HHG), infrared or visible light is upconverted into the extreme ultraviolet and soft-x-ray regions of the spectrum in a highly nonlinear parametric process [2]. However, during the HHG process the medium is ionized, and the associated strong plasma dispersion precludes true phase matching for conversion to photon energies  $> \sim 130$  eV [3]. Therefore, developing schemes for QPM is critical in extending efficient HHG conversion to soft-x-ray and shorter wavelengths. The first implementation of QPM to enhance HHG used modulated hollow waveguides to modulate the intensity of the driving laser, and therefore the HHG process [4–6]. This work succeeded in enhancing the conversion efficiency by 1–2 orders of magnitude, limited by inevitable variations in phase matching conditions (the coherence length) along the direction of propagation [7]. Recently, all-optical QPM using three counterpropagating pulses was used to enhance high harmonics around 70 eV by more than two orders of magnitude [8]. Since the all-optical approach allows for adaptive optimization to a varying coherence length, larger enhancements are expected when longer trains of counterpropagating pulses are used. This all-optical QPM approach is based on the fact that a weak counterpropagating field can suppress high harmonic emission in regions where it intersects with the driving pulse [9,10]. Thus, a sequence of  $N$  counterpropagating pulses can be used for implementing QPM by suppressing emission from  $N$  out-of-phase regions [8]. However, in all previous work, no quantitative model for QPM using counterpropagating pulse trains was formulated.

Here, we present a general model of QPM using counterpropagating pulse trains. A weak counterpropagating beam interferes with the driving laser and induces a sinusoidal modulation in the phase of the emitted harmonics. The amplitude of this phase

modulation is proportional to the square root of the intensity of the counterpropagating beam. These fast oscillations suppress the buildup of the harmonic signal, with a predicted suppression factor given by the zero-order Bessel function of the first kind of modulation amplitude. Negative values of the Bessel function correspond to flipping the phase of the generated harmonics, converting out-of-phase zones to in-phase zones. Consequently, we predict QPM efficiency factors that are greater than expected from simply suppressing harmonic emission from out-of-phase regions. Our model allows us to predict the optimal intensity and pulse shape of the counterpropagating pulse trains for implementing all-optical QPM at short wavelengths.

HHG is a highly nonlinear process that, under proper conditions, can result in coherent beams at extreme ultraviolet and soft-x-ray spectral wavelengths. In HHG, an intense driving laser first ionizes the atom and later accelerates the ionized electron in the continuum. A high energy photon is emitted when the energetic electron recombines with its parent ion. As a consequence of this noninstantaneous ( $\sim$ femtosecond) nonlinearity, the emitted harmonics are not phase locked with the driving laser. Remarkably, the phase shift  $\Delta\Phi$  acquired by the electron during its trajectory is linear in the laser intensity [11,12]. Consequently, modulating the laser intensity along the propagation direction  $z$ , through interference between the driving pulse and a counterpropagating beam, will result in a fast modulation of the phase shift  $\Delta\Phi$  given by [13]

$$\Delta\Phi(z) \propto \Delta I(z) \propto E_0^2 r \cos(2\pi z/\Lambda). \quad (1)$$

In Eq. (1),  $E_0$  is the peak field of the driving laser,  $r$  is the field ratio between the driving laser and the counterpropagating beam,  $\Lambda = \lambda/2$  is the periodicity of the intensity interference pattern, and  $\lambda$  is the wavelength of the laser beams, assumed here to be  $0.8 \mu\text{m}$ .

We first calculate the influence of a weak counterpropagating beam on the emitted harmonics and verify that sinusoidal oscillations in the phase of the

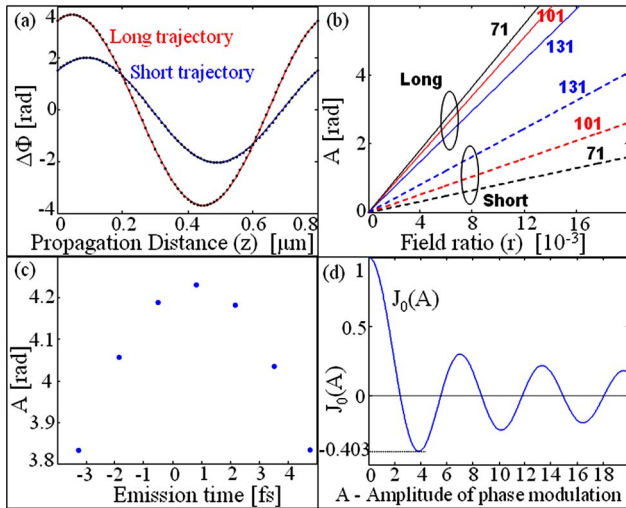


Fig. 1. (Color online) Influence of a weak counterpropagating field on the phase of the emitted harmonics. (a) Phase modulation of both the “short” and the “long” quantum paths for the 131st harmonic order (solid curves) by a counterpropagating beam for a driving laser intensity of  $10^{15}$  W/cm<sup>2</sup> and a counterpropagating laser intensity of  $10^{11}$  W/cm<sup>2</sup> in He. Fits to a cosine function (dotted curves) are also shown. (b) Calculated amplitude of the phase oscillations as a function of the ratio  $r$  between the peak fields of the backward- and forward-propagating beams. (c) Calculated amplitude of the phase oscillations of the long trajectory of harmonic order 101 as a function of the emission time with field ratio  $r=0.01$ . (d) Microscopic effective emission factor as a function of the phase modulation amplitude  $A$ .

emitted harmonics are induced [13]. Consider the superposition of forward- and backward-moving fields in the frame moving in the  $z$ -direction at the speed of light,  $c$ , given by  $E=E_0[\text{sech}(\tau/\tau_0)\cos(\omega\tau)+r\cos(\omega\tau+2kz)]$ , where  $k=2\pi/\lambda$  and  $\omega=ck$  are the angular wavenumber and frequency, respectively, and  $\tau_0$  is the driving pulse width. The amplitude of the emitted harmonics and their associated phase are calculated using the generalized Lewenstein model [14]. We find that the dominant effect of a low intensity counterpropagating beam is to induce changes in the harmonic phase, while the intensity of the emitted harmonic is much less sensitive to the weak counterpropagating beam. Figure 1 shows a typical result of such calculations, obtained for  $E_0=8.68\times 10^8$  V/cm ( $I_0=10^{15}$  W/cm<sup>2</sup>),  $\tau_0=11.36$  fs (FWHM is 20 fs), when the nonlinear medium is helium. As expected, the counterpropagating field induces a sinusoidal oscillation in the harmonic phase  $\Delta\Phi$ , with a periodicity  $\Lambda=\lambda/2=0.4\ \mu\text{m}$ . Figure 1(b) shows that the amplitude of the induced phase oscillation ( $A$ ) is indeed linearly proportional to the field ratio  $r$  between the driving and counterpropagating fields. Moreover, the amplitude of the phase modulation is larger for emission that results from the so-called long electronic trajectories that are influenced by the counterpropagating beam for longer times. [Harmonics generated in the plateau region result from short and long quantum trajectories. The short (long) paths correspond to electron trajectories in which the time between ionization and recombination is  $<3T/4$  ( $>3T/4$ ), where

$T=2.6$  fs is the optical cycle of the driving laser [15].] Also, the difference between the modulation amplitudes of the long and short trajectories decreases near cutoff (139th order), where the two trajectories merge. Figure 1(c) shows the dependence of the amplitude  $A$  on the emission time (different half-cycles of the driving laser) that results from the changing intensity of the driving field.

Next, we calculate the microscopic effective emission factor, which is the ratio between the generated harmonic fields without and with the presence of counterpropagating light, for one period of the standing wave ( $\Lambda$ ) [9]:

$$\xi = \frac{1}{\Lambda} \int_0^\Lambda \exp[i\Delta\Phi(z)] dz = \frac{1}{\Lambda} \int_0^\Lambda \exp\left[iA \cos\left(\frac{2\pi}{\Lambda}z\right)\right] dz = J_0(A). \quad (2)$$

In Eq. (2)  $J_0$  is the zero-order Bessel function of the first kind [Fig. 1(d)], and  $A$  is the amplitude of the induced phase modulation. Clearly, the counterpropagating field suppresses the harmonic emission,  $|\xi(A \neq 0)| < 1$ , in region that it intersects with the driving laser. Also, the microscopic effective emission factor can be negative, which corresponds to an extra  $\pi$  phase shift for HHG. Thus, the presence of a counterpropagating field can be used for flipping out-of-phase regions into in-phase regions, which for QPM is advantageous over just suppressing HHG generation in out-of-phase regions [8,9].

We are now in a position to formulate a general model for all-optical QPM using counterpropagating pulse trains. Consider emission of a single harmonic order from a single electron quantum pathway (the more general case may be studied by applying a linear superposition). The temporal profile of the counterpropagating pulse train maps directly onto the medium. Thus, it is possible to describe the pulse train by  $r(z)$ , the ratio between the driving and counterpropagating fields at some collision point  $z$ . The counterpropagating beam induces a fast phase oscillation in the emitted harmonic with an amplitude that is proportional to the field ratio  $A(z) \propto r(z)$ . The proportionality factor can be calculated numerically [as in Fig. 1(b)]. The harmonic field itself after some propagation distance  $L$  is given by

$$E_{HHG} = \int_0^L E_{HHG}^0(z) \exp\left[i\frac{\pi}{L_C(z)}z + A(z)\cos\left(\frac{2\pi}{\Lambda}z\right)\right] dz, \quad (3)$$

where  $E_{HHG}^0(z)$  and  $L_C(z)$  are the emitted harmonic field and coherence length without the presence of the counterpropagating light, respectively. We assume that  $L_C \gg \Lambda$ ,  $\Lambda(\partial L_C/\partial z) \ll L_C$ , and  $\Lambda(\partial E_{HHG}^0/\partial z) \ll E_{HHG}^0$ , which are reasonable assumptions except for extremely high-order harmonics that are not considered in this paper. (This is because variations in  $L_C$  and  $E_{HHG}^0$  result from loss of the driving laser, mode beating, and other mechanisms with characteristic length scales  $>100\ \mu\text{m}$ .) Under these conditions, it is possible to replace the sinu-

soidal phase modulation term in Eq. (3) with the microscopic effective emission factor to obtain

$$E_{HHG} \approx \int_0^L E_{HHG}^0(z) \xi[A(z)] \exp\left[i \frac{\pi}{L_C(z)} z\right] dz. \quad (4)$$

Equation (4) can now be used to evaluate the efficiency of QPM by counterpropagating pulse trains. For simplicity, we assume that  $L_C$  and  $E_{HHG}^0$  are  $z$ -independent (which is the case in a plasma waveguide for example [16]). First, we consider a sequence of secant hyperbolic pulses  $A(z) = A_0 \sum_n \text{sech}[(z - 2nL_C - L_C/2)/z_0]$ , where  $A_0$  and  $z_0$  are free parameters [Fig. 2(a), top]. Figure 2(a) shows the QPM efficiency factor, which is the generated signal at  $L \gg L_C$  normalized to the signal generated under perfect phase matching conditions  $\eta = |E_{HHG}(L)|^2 / (E_{HHG}^0 L)^2$ , versus  $A_0$  and  $z_0$ . The largest QPM efficiency factor, obtained for  $A_0 = 4.5$  rad and  $z_0 = 0.26L_C$ , is  $\eta = 0.14$ . This is 40% larger than the efficiency factor predicted for the case in which harmonic emission is completely eliminated from the out-of-phase regions, with no influence on the in-phase regions, which would be  $(1/\pi)^2 \approx 0.1$ . Further enhancement can be obtained using pulse shaping. Figure 2(b) shows the QPM efficiency factor when the counterpropagating beam consists of square pulses. The largest efficiency factor of  $\eta = 0.2$  is obtained for  $z_0 = L_C$  and  $A_0 = 0.403$ , which corresponds to the smallest value of  $J_0$  [Fig. 1(d)]. It is important to note that the results presented in Fig. 2 were calculated assuming a HHG field that is generated via either the short or the long quantum trajectories, but not both. Indeed, this is the typical condition in all-optical QPM, which can correct the phase mismatch for only one type of quantum trajectories [8]. However, if both the long and short trajectories contribute to the HHG field, then interference between the two paths probably decreases the QPM efficiency factor.

In conclusion, we present a semi-analytical model for quasi-phase matching of high harmonic generation using counterpropagating light. Our model predicts the optimal intensities and pulse shape of the

counterpropagating field and was used to evaluate the efficiency of all-optical QPM for secant hyperbolic and square pulse trains. We also demonstrate that the presence of the counterpropagating field can enhance HHG above what is predicted from simply suppressing emission from out-of-phase regions. This work opens the door to semi-analytical models of other light-induced QPM schemes for HHG, for example, phase matching via difference frequency mixing [17,18] and QPM fibers [4–6].

The authors gratefully acknowledge funding from the NSF ERC for EUV Science and Technology.

## References

1. M. M. Fejer, G. A. Magel, H. J. Dieter, and R. L. Byer, *IEEE J. Quantum Electron.* **28**, 2631 (1992).
2. H. C. Kapteyn, O. Cohen, I. P. Christov, and M. M. Murnane, *Science* **317**, 775 (2007).
3. A. Rundquist, C. G. Durfee III, Z. Chang, C. Herne, S. Backus, M. M. Murnane, and H. C. Kapteyn, *Science* **280**, 1412 (1998).
4. I. P. Christov, H. C. Kapteyn, and M. M. Murnane, *Opt. Express* **7**, 362 (2000).
5. A. Paul, R. A. Bartels, R. Tobey, H. Green, S. Weiman, I. P. Christov, M. M. Murnane, H. C. Kapteyn, and S. Backus, *Nature* **421**, 51 (2003).
6. E. A. Gibson, A. Paul, N. Wagner, R. Tobey, D. Gaudiosi, S. Backus, I. P. Christov, A. Aquila, E. M. Gullikson, D. T. Attwood, M. M. Murnane, and H. C. Kapteyn, *Science* **302**, 95 (2003).
7. A. L. Lytle, X. Zhang, J. Peatross, M. M. Murnane, H. C. Kapteyn, and O. Cohen, *Phys. Rev. Lett.* **98**, 123904 (2007).
8. X. Zhang, A. L. Lytle, T. Popmintchev, X. Zhou, H. C. Kapteyn, M. M. Murnane, and O. Cohen, *Nat. Phys.* **3**, 270 (2007).
9. J. Peatross, S. Voronov, and I. Prokopovich, *Opt. Express* **1**, 114 (1997).
10. S. L. Voronov, I. Kohl, J. B. Madsen, J. Simmons, N. Terry, J. Titensor, Q. Wang, and J. Peatross, *Phys. Rev. Lett.* **87**, 133902 (2001).
11. M. Lewenstein, P. Salieres, and A. L'huillier, *Phys. Rev. A* **52**, 4747 (1995).
12. Z. Chang, A. Rundquist, H. Wang, I. Christov, H. C. Kapteyn, and M. M. Murnane, *Phys. Rev. A* **58**, R30 (1998).
13. O. Cohen, X. Zhang, A. Lytle, T. Popmintchev, M. M. Murnane, and H. C. Kapteyn, *Phys. Rev. Lett.* **99**, 053902 (2007).
14. M. Geissler, G. Tempea, and T. Brabec, *Phys. Rev. A* **62**, 033817 (2000).
15. C. Kan, C. E. Capjack, R. Rankin, and N. H. Burnett, *Phys. Rev. A* **52**, 4336 (1995).
16. D. M. Gaudiosi, B. Reagan, T. Popmintchev, M. Grisham, M. Berrill, O. Cohen, B. Walker, M. M. Murnane, H. C. Kapteyn, and J. J. Rocca, *Phys. Rev. Lett.* **96**, 203001 (2006).
17. P. L. Shkolnikov, A. E. Kaplan, and A. Lago, *Opt. Lett.* **18**, 1700 (1993).
18. O. Cohen, T. Popmintchev, D. M. Gaudiosi, M. M. Murnane, and H. C. Kapteyn, *Phys. Rev. Lett.* **98**, 043903 (2007).

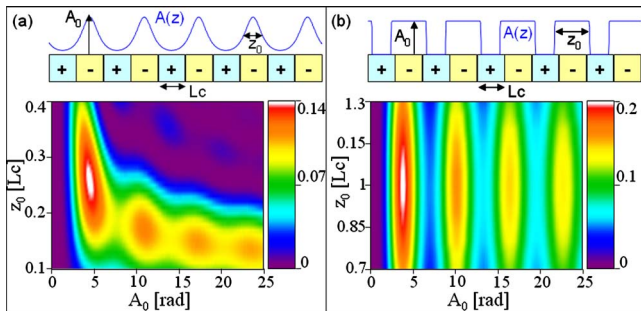


Fig. 2. (Color online) QPM efficiency factor for (a) a secant hyperbolic and (b) a square counterpropagating pulse train as a function of the pulse width and peak phase modulation amplitude. Note the different color scales in the two plots.